In Vivo Imaging of a New Indocyanine Green Micelle Formulation in an Animal Model of Laser-Induced Choroidal Neovascularization

Johanna Meyer,[1] Alexander Cunea,[1] Dagmar Sonntag-Bensch,[1] Pia Welker,[2] Kai Licha,[2] Frank G. Holz,[1] and Steffen Schmitz-Valckenberg[1]

[1]Department of Ophthalmology, University of Bonn, Bonn, Germany
[2]mivenion GmbH, Berlin, Germany

Correspondence: Steffen Schmitz-Valckenberg, Department of Ophthalmology, University of Bonn, Ernst-Abbe-Str. 2, 53127 Bonn, Germany; Steffen.Schmitz-Valckenberg@ukb.uni-bonn.de.

Submitted: November 22, 2013
Accepted: August 24, 2014

Citation: Meyer J, Cunea A, Sonntag-Bensch D, et al. In vivo imaging of a new indocyanine green micelle formulation in an animal model of laser-induced choroidal neovascularization. *Invest Ophthalmol Vis Sci*. 2014;55:6204–6212. DOI:10.1167/iovs.13-13617

Purpose. We investigated a novel formulation of indocyanine green (ICG/HS 15) in an animal model of laser-induced choroidal neovascularization (CNV).

Methods. The ICG was formulated with the nonionic solubilizer and emulsifying agent Kolliphor HS 15 to create ICG/HS 15 to improve the chemical stability and fluorescence efficacy. In vivo imaging was performed in rats that had undergone laser photocoagulation. Retinal uptake and fluorescence intensity of ICG and ICG/HS 15 were compared following intravenous injection of 3 dosages (0.05, 0.1, and 0.15 mg/kg body weight) at 7, 14, and 21 days following laser treatment. Postmortem analysis included histology with frozen sections and flat mounts.

Results. Immediately following injection of ICG or ICG/HS 15, a strong fluorescence was visible in the retinal vasculature and at the site of laser lesions. Pixel intensity was higher for ICG/HS 15 compared to conventional ICG at 8 minutes after injection for all different injection days and dosages. Over time, a continuous decrease of the fluorescent signal was observed for up to 60 minutes to baseline level. Flow cytometry data showed an increased uptake of micellar dye of macrophages and endothelial cells. Histology revealed an accumulation of the micellar dye within the laser lesion.

Conclusions. Micelle formulated ICG can be visualized in the retinal vasculature and laser-induced CNV in vivo and ex vivo. Micellar ICG/HS 15 showed in vivo stronger signal intensity when compared to ICG for all tested dosages. Following further investigations, ICG/HS 15 may be evaluated in patients with retinal and choroidal diseases for more refined diagnosis.

Keywords: indocyanine green, micellar formulation, micelles, Kolliphor, in vivo imaging, laser-induced choroidal neovascularization

The tricarbocyanine dye indocyanine green (ICG) is a water-soluble, protein-bound substance used for various diagnostic purposes.[1,2] A key advantage of ICG is the absorption and emission maxima in the near-infrared (600–900 nm) spectral range that allows for deep tissue penetration.[3] In case of overlying hemorrhages, the use of long wavelengths also is particularly helpful for the visualization of the underlying vasculature.[4] Common medical applications include visualization of blood flow in different organs and screening of inflammation in rheumatoid arthritis.[5–12] In ophthalmology, ICG has been used for both diagnostic purposes and surgical interventions.[13–16] For the former, intravenous injection of ICG into the blood enables retinal and choroidal angiography. It has proven useful in various retinal and macular diseases, including particular phenotypes of exudative age-related macular degeneration, such as occult choroidal neovascularization (CNV), retinal angiomatous proliferations (RAP), and polypoidal choroidal vasculopathy (PCV). The ICG-angiography procedure also is used in posterior uveitis syndromes. Finally, ICG has been introduced as a staining dye during vitrectomy for visualizing the internal limiting membrane (ILM) before peeling.[17]

Due to its chemical characteristics, ICG tends to form aggregates in aqueous solution, like dimers, oligomer, and polymers (depending on the concentration of the dye).[15,18–21] As a result, self-quenching of ICG subsequently occurs, causing reduced fluorescence efficacy. In aqueous solution, ICG exhibits a half-life of 16.8 ± 1.5 hours when stored in the dark (1 mg/L ICG). Due to strong protein binding and rapid uptake into the liver, ICG shows an initial half-life of 3 to 4 minutes when injected intravenously.[1,5,18] Using dynamic ICG angiography, Flower and Hochheimer[22,23] have taken advantage of these chemical characteristics to absolutely quantify the ICG concentration in the blood vessels at any time in vivo.

New developments in retinal imaging technology allow for better visualization with improved resolution and enhanced image contrast of the posterior pole of the eye in vivo. During recent years, in vivo imaging of rodents in experimental eye disease models by using the confocal scanning laser ophthalmoscopy (cSLO) has been applied increasingly.[24–29] For example, imaging of real-time retinal cell apoptosis[25] and laser-induced CNV has been reported.[30–34]

The aim of the current study was to develop a new formulation of ICG with better chemical stability and modified

fluorescence characteristics, and to test this molecule in vitro and in an animal model with in vivo and ex vivo correlations. The potentially better and longer visualization of this modified dye may be helpful for an improved detection and monitoring of pathological alterations in various eye diseases.

Materials and Methods

Animals

All procedures were approved by local authorities (Landesamt für Natur, Umwelt und Verbraucherschutz, Nordrhein-Westfalen, Germany, AZ 84-02.04.2011.A225) and complied with the Association for Research in Vision and Ophthalmology (ARVO) Statement for the Use of Animals in Ophthalmic and Vision Research. A total of 30 male adult Dark Agouti rats, each weighing 200 to 250 g, was anesthetized for all procedures by intraperitoneal injection of ketamine (60 mg/kg), and medetomidine hydrochloride (0.5 mg/kg). Supplemental anesthesia (ketamine and medetomidine hydrochloride) was administered intraperitoneally as needed. Ending of anesthesia was induced by intraperitoneal injection of a 20% atipamezol (1 mL/kg) solution. Topical 0.5% tropicamide (Mydriaticum Stulln; Pharma Stulln GmbH, Stulln, Germany) and 10% phenylephrine (Neosynephrin-POS; Ursapharm, Saarbrücken, Germany) eye drops were administered for pupillary dilation of both eyes.

Laser Photocoagulation

Retinal laser lesions were generated at day 0 to induce CNV formation. The animals were positioned before a slit-lamp laser delivery system. The fundus was visualized using a slide positioned on the cornea with 2% hydroxypropyl methylcellulose (OmniVision, Puchheim, Germany) as an optical coupling agent. An argon laser (Novus2000; Coherent, Dieburg, Germany) was used for photocoagulation (excitation, 514 nm; pulse duration, 0.1 second; laser power, 150 mW; and spot size setting, 100 μm). In all eyes, a series of six laser lesions were placed concentrically around the optic nerve head.

ICG Dyes

Two different ICG probes were investigated herein: the conventional, commercially available ICG dye (Pulsion, Feldkirchen, Germany) and a newly developed encapsulated ICG dye formulation. For the latter, ICG (Cardiogreen Standard Fluka; Sigma-Aldrich, Hamburg, Germany) was formulated with the nonionic solubilizer and emulsifying agent Kolliphor HS 15 (BASF, Ludwigshafen, Germany), also known as 2-hydroxyethyl 12-hydroxyoctadecanoate, to create ICG/HS 15 (mivenion GmbH, Berlin, Germany; Figs. 1A, 1B). Kolliphor HS 15 is amphiphilic, soluble in water, and exhibits a low toxicity and viscosity in rats and dogs.[35] One ICG molecule was encapsulated with 2000 molecules Kolliphor HS 15 to create a stable and spherical micelle (Fig. 1C). The micelles exhibit an average diameter of 13 nm.[36] The absorption maximum is at 798 nm, the emission maximum is at 825 nm (in aqua dest).

The ICG/HS 15 was prepared under sterile conditions and carried over in phosphate-buffered saline solution (PBS). After encapsulating ICG with Kolliphor HS 15, the dye was lyophilized by the manufacturer (mivenion GmbH). Lyophilized ICG/HS 15 was stored at 2° to 6°C. Both dyes were reconstituted on the day of injection to a concentration of 1 mg/mL with distilled water (Ampuwa; Fresenius Kabi, Bad Homburg, Germany).

A low, medium, and high dose (0.05, 0.1, and 0.15 mg/kg body weight [b.w.], respectively) for conventional ICG and ICG/HS 15 were each tested in five individual animals ($n = 30$), respectively (Tables 1, 2). Each animal underwent serial intravenous injection of the identical dye and concentration followed by in vivo fluorescence imaging at days 7, 14, and 21.

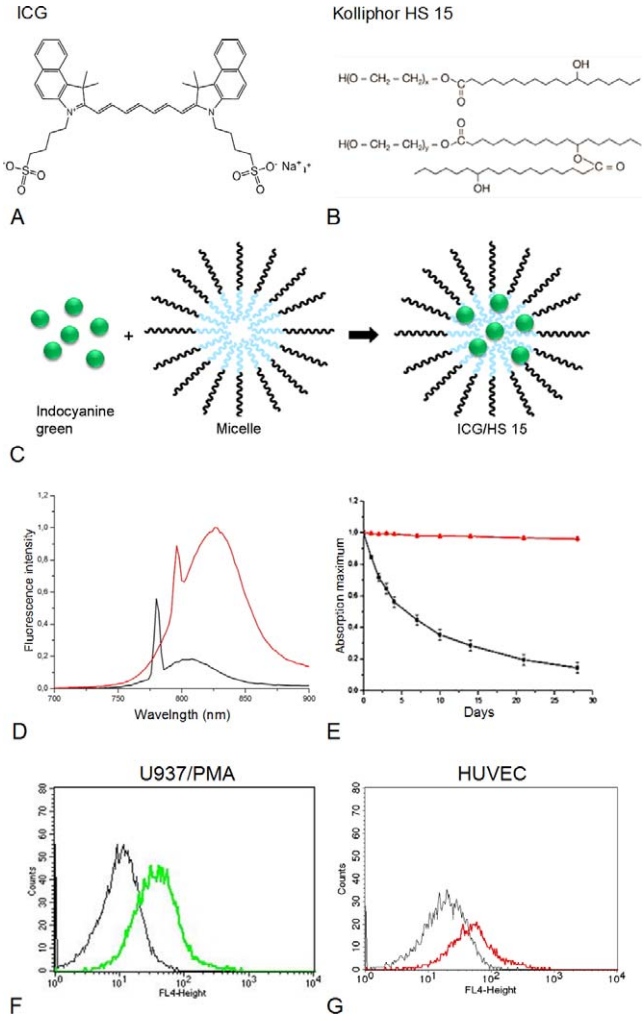

Figure 1. In vitro testing of ICG and ICG/HS 15. Chemical structures of ICG (**A**) and Kolliphor HS 15 (**B**). The ICG was formulated (**C**) with the amphiphile solubilizer Kolliphor HS 15 to create ICG/HS 15. Fluorescence intensity (**D**) of ICG/HS 15 is increased compared to conventional ICG (for accurate comparison, excitation wavelengths of both dyes were corresponding to absorption maxima, respectively). Also the chemical stability (**E**) of ICG/HS 15 in aqueous solution was increased for up to 30 days in contrast with a chemical stability for 1 day of conventional ICG. For immunohistochemical analysis micellar Dye700/HS 15 was used. Analysis of FACS showed an uptake of Dye700 (*black*) and micellar formulated Dye700/HS 15 (*green*) when cultured with U937/PMA (a human macrophage cell line [**F**]) and HUVEC cells (**G**). Fluorescence-activated cell sorting results (**D**–**G**) were measured in buffer solution with identical dye concentrations.

Fluorescence-Activated Cell Sorting (FACS)

For cellular studies, Dye700 (mivenion GmbH), a dicarbocyanine analogue to ICG, was encapsulated into Kolliphor HS 15 and used for microscopy and FACS studies (absorption maximum 685 nm, fluorescence emission maximum 715 nm). Human hematopoietic cell line U937 was routinely propagated as follows: RPMI medium, with 10% fetal calf serum (FCS) and penicillin/streptomycin (all from PAN-Biotech, Aidenbach, Germany) was added. Cells were seeded

Table 1. Qualitative Analysis of the In Vivo Images Illustrating the Time Period of Visible Fluorescence in the Retinal Vessels (Using In Vivo Images at +12 D) After Injection of Conventional ICG or ICG/HS 15 (Mean Time Point for all Tested Days Following Photocoagulation)

Tested Dye	Concentration	Dosage, mL	Dosage Level	Time Period of Visible Fluorescence in Retinal Vessels, Mean Min				
				D7	D14	D21	Median	*P* Value
ICG	0.05 mg/kg b.w.	0.2	Low	50	55	50	51.78	0.004
ICG/HS 15				60	60	60	60	
ICG	0.1 mg/kg b.w.	0.4	Medium	60	60	60	60	0.15
ICG/HS 15				60	60	60	60	
ICG	0.15 mg/kg b.w.	0.6	High	60	60	60	60	0.77
ICG/HS 15				60	60	60	60	

Statistical analysis was calculated with Mann-Whitney *U* test. D, days following laser treatment.

into medium at 1×10^5 cells/mL, cultured at 37°C with 5% CO_2, and split 1:30 two times a week. The U937 cells were differentiated toward the macrophage phenotype by incubation with 10 nM phorbol myristate acetate (PMA; Calbiochem, San Diego, CA, USA) for 5 days (U937/PMA). Human umbilical vein endothelial cells (HUVEC) were cultured in endothelial cell growth medium with supplement-mix (PromoCell GmbH, Heidelberg, Germany). This investigation was carried out according to the principles outlined in the Declaration of Helsinki for medical research involving human subjects (2008). Cells were seeded into medium at 2×10^4 cells/mL, cultured at 37°C with 5% CO_2 up to 80% of confluence and then split 1:4.

For FACS analysis, 2×10^5 cells/mL cells were cultured in 24-well plates with normal culture medium or medium containing 10^{-6} M test substance for 3 hours. Thereafter, cells were washed with PBS and detached with 200 µL/well accutase (PAA) and washed two times with PBS. Cells were fixed with 500 µL 3% paraformaldehyde for 10 minutes at 4°C, stopped with 2 mL PBS and centrifuged at 250*g*, for 10 minutes at 4°C. Supernatants were removed and cells were suspended in 200 µL PBS with 0.5% bovine serum albumin (Carl Roth GmbH & Co. KG, Karlsruhe, Germany). Fixed cells were kept at 4°C until analyzed in a FACS Calibur analysis instrument (Becton-Dickinson, East Rutherford, NJ, USA).

In Vivo Imaging With Scanning Laser Ophthalmoscope

All images were performed using confocal scanning laser ophthalmoscopy (HRA2; Heidelberg Engineering, Heidelberg, Germany). Anesthetized animals were placed on a customized platform in front of the camera lens. A heat pad together with an animal rectal probe was used to ensure constant body temperature at approximately 37°C. A 55° lens was used to achieve wide field images (all degree values calibrated for the human eye). Both eyes were imaged successively in the near infrared reflectance and near infrared fluorescence mode in a single and standardized session to compare different dyes and their concentrations. For near-infrared fluorescence imaging, the laser power was set at 100% (approximately 2.7 mW) and the detector sensitivity at 92% (high resolution mode), respectively. To improve the signal-to-noise ratio and to enhance image contrast, a mean image of a series of single images (100 frames acquired over 21.28 seconds) was calculated after correction of body movements. Fluorescence images were taken before dye injection and at predefined time points following dye injection (2, 4, 6, 8, 10, 20, 30, 40, 50, and 60 minutes, and 24 hours). At each time point, images with four different focus settings (+12, +8, +4, and 0 diopters [D]) were obtained. Using the confocal optics, this approach allows for the acquisition of sectional scans through the rat retina for investigation of the depth location of the detected fluorescence signal.

To prevent cataract formation and optimize image clarity, lubricating eye drops (Oculotect fluid 50 mg/mL; Novartis Pharma, Nürnberg, Germany) were placed on the eyes every 1 to 2 minutes. In vivo imaging was followed by topical administration of Corneregel (Bausch & Lomb, Berlin, Germany).

Image Analysis

The pharmacokinetics with the fluorescence characteristics for both dyes and their three different concentrations were evaluated. Identical time points (prior, and 8, 22, 32, 42, 52, 62 minutes, and 24 hours following dye application) were compared. Fluorescence intensity within major retinal blood vessels, inside the laser lesions, and the background was specifically analyzed. In addition, the visibility of fluorescence in large choroidal vessels within the background was determined. For quantitative analysis, nonnormalized images were processed and their pixel intensity analyzed. Images with

Table 2. Qualitative Analysis of the In Vivo Images Illustrating the Time Period of Visible Fluorescence in the Choroidal Vessels (Using In Vivo Images at +4 D) After Injection of Conventional ICG or ICG/HS 15 (Mean Time Point for all Tested Days Following Photocoagulation)

Tested Dye	Concentration	Dosage, Ml	Dosage Level	Time Period of Visible Fluorescence in Choroidal Vessels, Mean Min				
				D7	D14	D21	Median	*P* Value
ICG	0.05 mg/kg b.w.	0.2	Low	7	5.6	6	6	0.0001
ICG/HS 15				17.4	25.6	15.2	19	
ICG	0.1 mg/kg b.w.	0.4	Medium	5.6	5.4	5.6	6	0.0001
ICG/HS 15				24.8	24	25.4	24	
ICG	0.15 mg/kg b.w.	0.6	High	7.4	6.4	6.8	7	0.0001
ICG/HS 15				23.6	28.6	29.6	27.67	

Statistical analysis was calculated with Mann-Whitney *U* test.

Investigative Ophthalmology & Visual Science

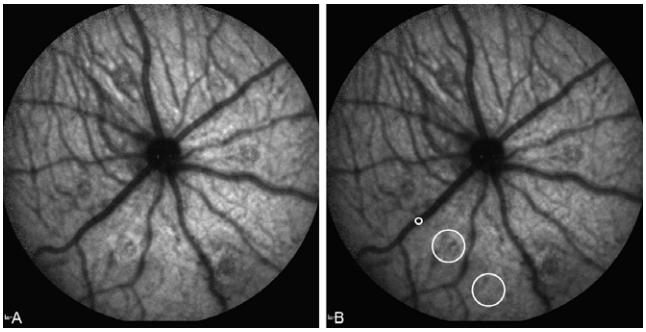

FIGURE 2. Near-infrared fluorescence in vivo imaging of the rat eye before dye application showing ill-defined retinal laser lesions at day 7 following laser treatment ([**A**], *native image*). For analysis of fluorescence signal, pixel intensities were determined. (**B**) The standardized size of circles that were placed manually at the site of retinal vessels (*small circle*) as well as at the site of the laser lesions and background fluorescence (*larger circles* with identical size) after image acquisition.

a focus setting of +12 D were used for the measurement of pixel intensity of the retinal vessels. For the examination of the background and laser lesions, images at +4 D were utilized.[25] Pixel intensity analysis was achieved by placing a circle at the region of interest (Fig. 2A) using Photoshop CS5 (Adobe Systems, San Jose, CA, USA).[37,38] The size of the circle had a diameter of 70 pixels for retinal blood vessels, 26,000 pixels for laser lesions, and 26,000 pixels for the background. No exact scaling for imaging the eye of dark Agouti rats with the cSLO is established. A rough estimation would be that the size of 26,000 pixels corresponds to 0.041 mm^2. This calculation is based on the assumption that the circle size for the laser lesions and the background is similar to size of the optic nerve head.[39,40] The circle for background and laser lesion analysis was defined as an area outside laser lesions and with no major retinal blood vessels. The intensity of the fluorescence signal then was measured in gray scale arbitrary units (values from 0–255) as the averaged value of all pixel units within the dedicated circle. For further analysis, the mean zero gray level[41] was subtracted from each of the measurements.

For statistical analysis, differences were evaluated by the Mann-Whitney *U* Test using SPSS software (PASW Statistics 20; SPSS, Inc., Chicago, IL, USA). The results were expressed as the mean ± SD and $P < 0.05$ was considered as statistically significant.

Histology and Immunohistochemistry

For histology, animals were euthanized using 100% carbonic acid gas and eyes were enucleated immediately. Due to the technical difficulties to visualize the fluorescent dye localization at high-resolution in the near-infrared range using fluorescence microscopy,[38] animals for immunohistochemistry received 0.1 mg/kg b.w. solution of Dye700/HS 15 (mivenion GmbH) 10 minutes before enucleation (day 7 following laser treatment).

Eyes were embedded in OCT (Tissue Tek; Sakura Finetek Europe B.V., Alphen aan den Rijn, Netherlands) for frozen sections and cut into 10 µm sections. Frozen sections were mounted on a glass slide, fixed with 100% methanol and stained with 4′,6-diamidino-2-phenylindole dihydrochloride (DAPI, Dapi BioChemica; AppliChem GmbH, Darmstadt, Germany), CD68 (mouse anti CD68 IgG1 Clone ED1; Acris Antibodies GmbH, Herford, Germany), Iba1 (polyclonal anti Iba1, rabbit; Wako Chemicals GmbH, Neuss, Germany), or von Willebrand factor (vWF, polyclonal rabbit anti-human; Dako Cytomation, Glostrup, Denmark).

Additionally to light microscopy, some eyes were processed for retinal and sclerochoroidal flat mounts as described previously[42] and examined with fluorescence microscopy. Following enucleation and fixation, eyes were washed (in 0.1 mol PBS) and the anterior part was removed. The retina and choroid were separated. Both segments were incubated with vWF at 4°C overnight (dilution of 1:10,000). The next, flat mount sections were incubated for one hour at room temperature with Alexa Fluor488 goat anti-rabbit IgG (Invitrogen Molecular Probes, Eugene, OR, USA) for vWF staining (dilution of 1:150). Finally, flat mounts were rinsed and cover slips were placed over the segments with Shandon Immu-Mount medium (Thermo Scientific, Fisher, UK). All fluorescent images were collected from an Olympus fluorescence microscope (IX71; Olympus, Hamburg, Germany) using a ×10 or ×40 objective and filter set for a fluorescein set (excitation filter wavelength, 480/40 nm; emission filter wavelength, 535/50 nm) and a set for Dye700 (excitation filter wavelength, 660 nm; emission filter wavelength, 700/40 nm).

Results

Properties of ICG/HS 15 and In Vitro Experiments

Encapsulating of ICG with Kolliphor HS 15 (Figs. 1A–C) was achieved to improve the chemical stability and fluorescence efficacy of ICG in aqueous solution. ICG/HS 15 demonstrated in vitro a twice higher fluorescence intensity measured by FACS than conventional ICG (Fig. 1D). The maximum of fluorescence intensity of ICG/HS 15 exhibited a shift to longer wavelengths compared to conventional ICG (Fig. 1D). Also the chemical stability in aqueous solution (Fig. 1E) of ICG/HS 15 was increased for up to 30 days in contrast to 1 day for conventional ICG. In addition, analysis of FACS data showed an increased uptake of micellar Dye700/HS 15 comparing to free Dye700 of U937/PMA macrophages and HUVEC endothelia cells in vitro (Figs. 1F, 1G).

In Vivo Imaging and Pharmacokinetics

In vivo imaging before dye application showed ill-defined retinal lesions at the site of laser damage (Figs. 2, 3), but no fluorescence signal was detectable. Following dye application, a strong fluorescence was immediately visible (Fig. 3) with slow decline in fluorescence intensity over time. This observation was made with both dyes at all three tested concentrations and at all three tested time points after laser treatment, although variations in the signal strength and the duration of any detectable fluorescence following injection were found (Fig. 3; Tables 1, 2).

The strongest fluorescence was visible within major retinal vessels that immediately occurred; that is, it was detected at the earliest time point (60 seconds). At the site of laser lesions, a slightly weaker fluorescence signal with a halo-like appearance was observed a couple of minutes following dye injection. Typically, the center itself remained unstained surrounded by a hyperfluorescence ring (Fig. 3). Furthermore, a weak fluorescence of the background that presumably originated from the choroid was observed. The latter fluorescence initially was visible at 60 seconds. However, it disappeared much faster compared to the fluorescence signal within retinal vessels and at the site of laser lesions. For the higher dye concentrations, even large choroidal vessels could be distinguished up to 7 minutes for conventional ICG and 28 minutes after injection of ICG/HS 15 (Table 2).

Comparing different concentrations of the same dye, the qualitative assessment revealed that higher dosages always

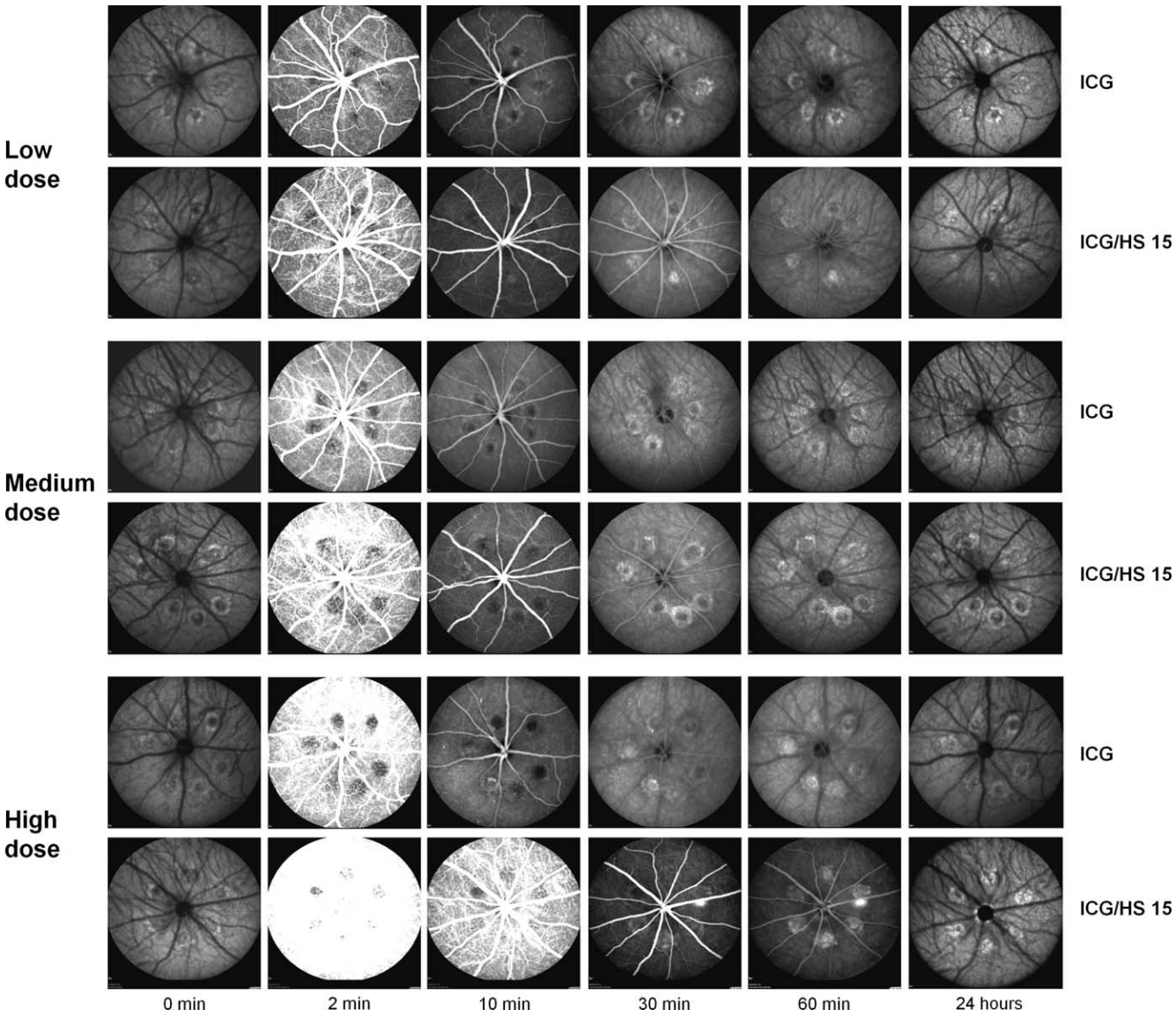

FIGURE 3. In vivo imaging and pharmacokinetics of different dye concentrations. Staining of conventional ICG (*first*, *third*, and *fifth rows*) or ICG/HS 15 (*second*, *fourth*, and *sixth rows*) was observed 14 days following laser treatment in vivo with the cSLO (standardized settings, all images were taken at +12 D). Representative angiograms shown here illustrating staining before dye injection, and approximately 2, 10, 30, and 60 minutes after intravenous dye injection, as well as 24 hours following dye injection. The ICG/HS 15 showed qualitatively an overall brighter fluorescence compared to conventional ICG.

were correlated with higher signal strength and longer observation of detectable fluorescence signal within retinal vessels, laser lesions, and the background (for details, see Tables 1, 2). Comparing directly ICG to ICG/HS 15 with identical dye concentrations, the stronger and longer visible fluorescence always was seen with ICG/HS 15 (Fig. 3; Tables 1, 2). No matter what concentration or dye tested, no clear difference in the decay of fluorescence was seen.

Quantitative Analysis of In Vivo Fluorescence

The more detailed quantitative analysis (Fig. 4) of mean pixel intensities at the sites of retinal vessels, laser lesions, and the background did confirm the qualitative observations. The fluorescence intensity always was higher for ICG/HS 15 compared to conventional ICG at all three time points. Even the signal intensity for the low ICG/HS 15 dosage was higher compared to the high dosage of conventional ICG (Fig. 4). The fluorescence overall was much more pronounced after 8 minutes compared to 62 minutes following intravenous dye injection as well as for the signal within retinal vessels (Fig. 4A) compared to the similar signal strength of laser lesions (Fig. 4B) and the background (Fig. 4C). At 8 minutes, an obvious dose-dependent increase in signal intensity at the site of the laser lesions and in the background for both dyes was observed with higher dye concentrations. Corresponding to retinal vessels (Fig. 4A), the signal strength of ICG/HS 15 already was close to the maximum possible pixel values at the lowest dose. No clear increase in signal intensity with higher dosage was seen (using the standardized settings for laser power and detector sensitivity). In contrast, a dose-dependent increase in signal strength (Fig. 4A) was observed within the retinal vessels for conventional ICG.

The differences between ICG/HS 15 and ICG leveled off over time. At 20 minutes, there still was a trend for higher fluorescence for ICG/HS 15 with almost no difference after 40

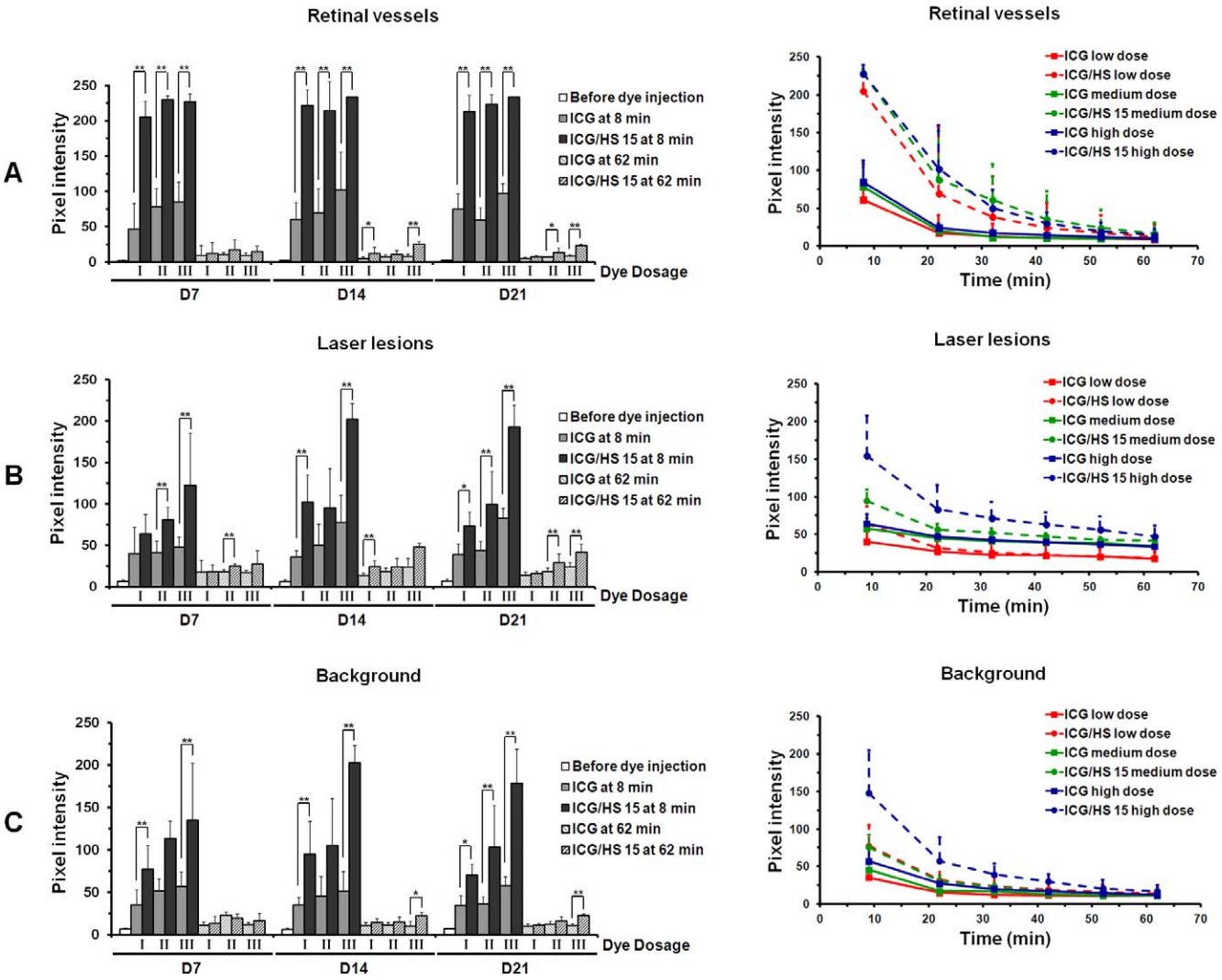

Figure 4. Quantitative analysis of signal intensities for ICG and ICG/HS 15 at 8 and 62 minutes for all three concentrations and time points following laser treatment. D7, day 7; D14, day 14; D21, day 21. Signal intensity was separately evaluated for three anatomical sites ([**A**], retinal vessels; [**B**], laser lesions; and [**C**], background). The three tested dye dosages are labeled as I = 0.05, II = 0.1, and III = 0.15 mg/kg b.w. Pixel intensity immediately before dye injection was determined and showed normalized fluorescence. Progress of pixel intensity determined for a low (*red*), medium (*green*), and high (*blue*) dose of ICG (*continuous bar*), and ICG/HS 15 (*dotted bar*) at day 7 following laser treatment. Overall highest pixel intensity was observed with ICG/HS 15 compared to conventional ICG, regardless of the tested dosage. Highest pixel intensity in all analyzed regions was demonstrated with highest dosage of ICG/HS 15, and lowest pixel intensity with low dose of ICG. Over time, a continuous decrease of the fluorescent signal was observed for up to 60 minutes and pixel intensities at 62 minutes were adjusted to baseline values. Statistical analysis was performed using the Mann-Whitney *U* test with $^{*}P \leq 0.05$ and $^{**}P \leq 0.05$. The results were expressed as the mean ± SD.

to 50 minutes following dye application, reaching the range of the baseline fluorescence intensity values. No fluorescent signal was detectable 24 hours after dye application for a low, medium, or high dosage of either ICG/HS 15 or ICG (Fig. 3), regardless of dye concentration and day of application.

There were only subtle differences of the fluorescence intensity for ICG and ICG/HS 15, and for the identical concentrations between different days after laser treatment (Fig. 4).

Histology and Immunohistochemistry

Immunohistochemistry of frozen cross-sections as well as retinal and choroidal flat mounts showed accumulation of the micellar formulated Dye700/HS 15, used here as analogue to ICG/HS 15 due to the better ability of detection in the microscope setting, within the laser lesions and choroid (Fig. 5A). The macrophage marker CD68 (Fig. 5B) as well as the microglia marker Iba1 (Fig. 5C) were correlated with Dye700/HS 15 accumulation within laser lesion and the choroidal layer. In addition, free and nonphagocytized Dye700/HS 15 also was visible. Neither colocalization of Dye700/HS 15 after staining with anti-cytoceratin (CKpan, data not shown) nor colocalization of Dye700/HS 15 after staining of blood vessels with vWF was detectable (Fig. 5D). Frozen cross-section of liver, spleen, and kidney also showed an accumulation of Dye700/HS 15, illustrating the pharmacokinetics of micellar formulated Dye700 and the retention via kidney and liver (Supplementary Fig. S1). Immunohistochemical analysis of retinal and choroidal flat mounts (Fig. 5E) revealed accumulation of Dye700/HS 15 within the laser lesions, while the signal at the level of the choroid was much stronger compared to the intensity seen at the level of the retina. Endothelial staining with vWF showed dye accumulation with the choroid and retinal vessels, but not within laser lesions at the level of the retina.

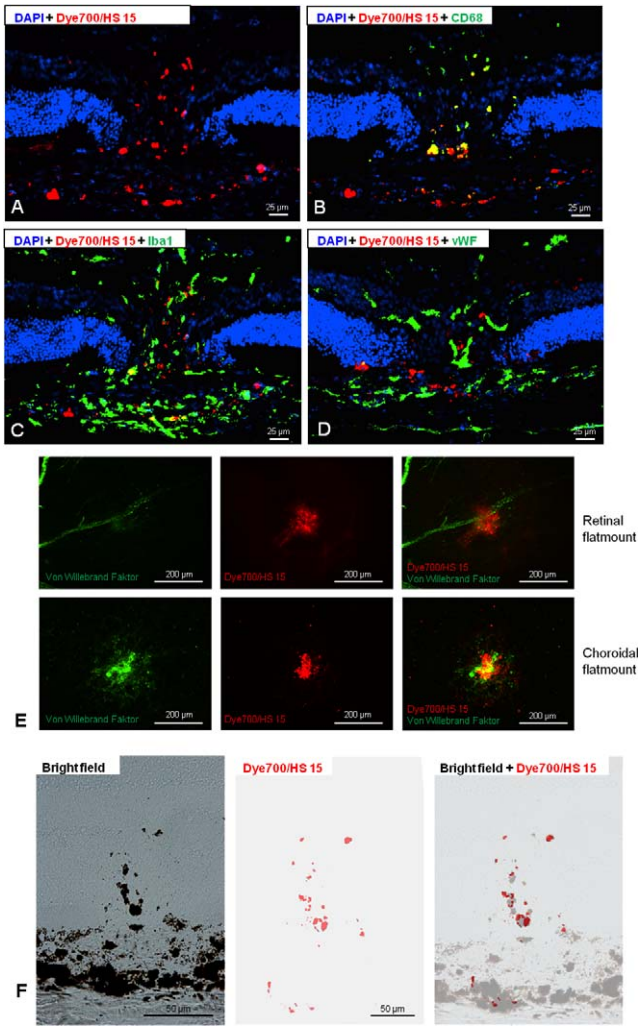

Figure 5. Ex vivo analysis of Dye700/HS 15 (in *red*) accumulation 7 days following laser treatment. A staining of Dye700/HS 15 within the laser lesions was detected in frozen sections (**A–C**) as well as in flat mount preparations (**E**). Frozen sections were stained with DAPI (*blue*) (**A**), CD68 (**B**), Iba1 (**C**), and vWF ([**D**], all in *green*). Colocalizations of Dye700/HS 15 with CD68 as well as Iba1 were observed in the site of laser lesion and choroid, but also free dye in the laser lesion was visible. No colocalization of Dye700/HS 15 after staining of blood vessels with vWF was detectable in the frozen section as well as in the retinal (*first row*) and choroidal (*second row*) flat mounts. (**E**). Staining of neovascular retinal vessels with Dye700/HS 15 is moderate (*first row, last picture*), but an intense staining of the new choroidal vessels (*second row, last picture*) could be observed. An overlay of bright field image and Dye700/HS 15 frozen section image exhibited the staining of the laser lesion and choroid (**F**). All images were taken using fluorescence microscopy with ×40 (**A–E**) and ×10 (**F**) magnification.

A bright field image of a frozen section showed pigmented agglomerates at the site of laser lesions, which were positive for CD68 (Fig. 5F). The overlay of the latter with a frozen section disclosed a colocalization of CD68-positive macrophages and Dye700/HS 15.

Discussion

The results demonstrated that micellar formulated ICG can be visualized in vivo in the retinal vasculature and within laser lesions, showing overall higher signal intensities compared to conventional ICG for all tested dosages at all tested days (Figs. 4, 5; Tables 1, 2). These observations are in accordance with the chemical properties of this new formulation that, due to its micellar formulation, is characterized by an increased distance between single ICG molecules avoiding clustering and formation of ICG aggregates.[15,18,20] Subsequently, quenching phenomena are largely reduced leading to a more intense fluorescence signal.[36] The additional longer staining of retinal and choroidal vessels over time would be consistent with an improved fluorescence quantum yield in the circulation. The decay kinetics suggest that ICG/HS 15 enters the same clearance pathway of excretion via the liver (Supplementary Fig. S1) compared to conventional ICG. An effect of the micellar formulation on the pharmacokinetic parameters of ICG in blood cannot be derived from the investigation and would require quantification of the ICG concentration by chemical analytical methods. Immunohistochemical analysis revealed the ability of micellar formulated Dye700/HS 15 for staining the laser lesions as well as the vasculature (Fig. 5). A colocalization with Dye700/HS 15 and macrophages, as well as microglia within the laser lesion was observed.

In vivo experiments were carried out in pigmented rats using standardized imaging protocols, and including qualitative and quantitative analyses. For the latter, pixel intensities of both dyes at predefined time points were determined and the mean gray value of all areas of interests was calculated.[37,38,41] Therefore, we found apparent differences between ICG and ICG/HS 15, while only relatively slight variations were seen for identical setups (i.e., dyes, dosages, time points). Particularly at the start of the dye transit, ceiling effects (in the sense of blooming/saturation of the digital images) occurred using the predefined settings that were chosen to cover the broad range of fluorescence between different setups. The imaging protocol includes dye injection, immediately followed by careful positioning and camera alignment, allowed for standardized in vivo fluorescence imaging at high quality as early as possible at 8 minutes after injection, while the systematic assessment of the filling phase was not possible. Overall, it remains unclear if the filling phase in an animal model that notably has no macula would be comparable to a future potential application in humans.

Previous studies have shown an increased fluorescence of (modified) ICG after encapsulating or coating the dye.[36,38,43–47] Kolliphor HS 15, which was used in this study, has been tested broadly as surfactant in drug formulation, and has shown high tolerability and safety in many biological systems.[48–50] These reports are in accordance with no observations of any toxic effects of micellar formulated ICG or Dye700 in vivo (Fig. 3) or ex vivo (Fig. 5, Supplementary Fig. S1).

Indocyanin green is used for fluorescence angiography in ophthalmology in clinical routine and for research application.[14,22] Quenching phenomena of ICG have been used by Flower and Hochheimer[22,23] to absolutely quantify the ICG concentration in the blood vessels at any time in vivo. The findings of this study would imply that the amount of dye may be reduced in a potential human application with the encapsulated ICG/HS 15, yielding an equal fluorescence compared to higher doses of conventional ICG. Using identical dye concentrations, ICG/HS 15 may be visible longer. At the same time, it appears conceivable that the lack of tissue staining that has been regarded as an advantage of conventional ICG is preserved. This assumption is supported by the observation that no fluorescence of ICG/HS 15 was visible 24 hours after dye injection.

The highest dose of ICG used in this study in rats roughly corresponds to the well-established concentration for ICG angiography in humans. According to the user information for ICG (Pulsion) the recommended dosage is 0.1 to 0.3 mg/kg b.w. Based on our results (Fig. 4), we would estimate that the

Investigative Ophthalmology & Visual Science

potentially required dose of ICG/HS 15 for fluorescence angiography in patients would be in the order of two-thirds lower compared to ICG (Fig. 4A).

Upon further investigations in animal models, ICG/HS 15 opens potential applications in patients with various retinal and choroidal diseases[14] for more refined diagnosis. A clinical pilot-study testing micellar ICG/HS 15 in humans and the possible ophthalmological application is planned.

Acknowledgments

The authors thank Claudine Strack for technical assistance with histology and helpful discussions.

Supported by the German Ministry of Education and Research (BMBF), FKZ 13N10349.

Disclosure: **J. Meyer**, None; **A. Cunea**, None; **D. Sonntag-Bensch**, None; **P. Welker**, mivenion GmbH (E); **K. Licha**, mivenion GmbH (E), P; **F.G. Holz**, Acucela (C), Allergan (C), Genentech (F), Heidelberg Engineering (F), Carl Zeiss Meditec (F), Novartis (F, C), Optos (F), Merz (C), Bayer (F, C), Boehringer Ingelheim (C); **S. Schmitz-Valckenberg**, Heidelberg Engineering (C, F, R), Optos (F), Carl Zeiss Meditec (F), Genentech (C), Novartis (F, C, R), Roche (C,R)

References

1. Landsman ML, Kwant G, Mook GA, Zijlstra WG. Light-absorbing properties, stability, and spectral stabilization of indocyanine green. *J Appl Physiol*. 1976;40:575–583.
2. Taichman GC, Hendry PJ, Keon WJ. The use of cardio-green for intraoperative visualization of the coronary circulation: evaluation of myocardial toxicity. *Tex Heart Inst J*. 1987;14:133–138.
3. Licha K, Olbrich C. Optical imaging in drug discovery and diagnostic applications. *Adv Drug Deliv Rev*. 2005;57:1087–1108.
4. Yannuzzi LA, Slakter JS, Sorenson JA, Guyer DR, Orlock DA. Digital indocyanine green videoangiography and choroidal neovascularization. *Retina*. 1992;12:191–223.
5. Caesar J, Shaldon S, Chiandussi L, Guevara L, Sherlock S. The use of indocyanine green in the measurement of hepatic blood flow and as a test of hepatic function. *Clin Sci*. 1961;21:43–57.
6. Paumgartner G, Probst P, Kraines R, Leevy CM. Kinetics of indocyanine green removal from the blood. *Ann N Y Acad Sci*. 1970;170:134–147.
7. Hauptman JG, DeJong GK, Blasko KA, Chaudry IH. Measurement of hepatocellular function, cardiac output, effective blood volume, and oxygen saturation in rats. *Am J Physiol*. 1989;257:R439–R444.
8. Werner SG, Langer HE, Ohrndorf S, et al. Inflammation assessment in patients with arthritis using a novel in vivo fluorescence optical imaging technology. *Ann Rheum Dis*. 2012;71:504–510.
9. Schaafsma BE, Mieog JS, Hutteman M, et al. The clinical use of indocyanine green as a near-infrared fluorescent contrast agent for image-guided oncologic surgery. *J Surg Oncol*. 2011;104:323–332.
10. Ntziachristos V, Yodh AG, Schnall M, Chance B, Concurrent MRI. and diffuse optical tomography of breast after indocyanine green enhancement. *Proc Natl Acad Sci U S A*. 2000;97:2767–2772.
11. Ergin A, Wang M, Zhang JY, et al. The feasibility of real-time in vivo optical detection of blood-brain barrier disruption with indocyanine green. *J Neurooncol*. 2012;106:551–560.
12. Ozgiray E, Akture E, Patel N, et al. How reliable and accurate is indocyanine green video angiography in the evaluation of aneurysm obliteration? *Clin Neurol Neurosurg*. 2013;115:870–878.
13. Spaide RF, Yannuzzi LA, Slakter JS, Sorenson J, Orlach DA. Indocyanine green videoangiography of idiopathic polypoidal choroidal vasculopathy. *Retina*. 1995;15:100–110.
14. Dithmar S, Holz FG. *Fluoreszenzangiographie in der Augenheilkunde*. Heidelberg, Germany: Springer Medizin Verlag; 2008.
15. Desmettre T, Devoisselle JM, Mordon S. Fluorescence properties and metabolic features of indocyanine green (ICG) as related to angiography. *Surv Ophthalmol*. 2000;45:15–27.
16. Slakter JS, Yannuzzi LA, Guyer DR, Sorenson JA, Orlock DA. Indocyanine-green angiography. *Curr Opin Ophthalmol*. 1995;6:25–32.
17. Burk SE, Da Mata AP, Snyder ME, Rosa RH Jr, Foster RE. Indocyanine green-assisted peeling of the retinal internal limiting membrane. *Ophthalmology*. 2000;107:2010–2014.
18. Saxena V, Sadoqi M, Shao J. Degradation kinetics of indocyanine green in aqueous solution. *J Pharm Sci*. 2003;92:2090–2097.
19. Holzer W, Mauerer M, Penzkofer A, et al. Photostability and thermal stability of indocyanine green. *J Photochem Photobiol B*. 1998;47:155–164.
20. West W, Pearce S. The dimeric state of cyanine dyes. *J Phys Chem*. 1965;69:1894–1903.
21. Zhou JF, Chin MP, Schafer SA. Aggregation and degradation of indocyanine green. In: Anderson RR, ed. *Proc. SPIE 2128. Laser Surgery: Advanced Characterization, Therapeutics, and Systems IV*. Los Angeles, CA: R. Rox Anderson; 1994:495–505.
22. Flower RW, Hochheimer BF. A clinical technique and apparatus for simultaneous angiography of the separate retinal and choroidal circulations. *Invest Ophthalmol*. 1973;12:248–261.
23. Flower RW, Hochheimer BF. Quantification of indicator dye concentration in ocular blood vessels. *Exp Eye Res*. 1977;25:103–111.
24. Eter N. Molecular imaging in the eye. *Br J Ophthalmol*. 2010;94:1420–1426.
25. Schmitz-Valckenberg S, Guo L, Maass A, et al. Real-time in vivo imaging of retinal cell apoptosis after laser exposure. *Invest Ophthalmol Vis Sci*. 2008;49:2773–2780.
26. Seeliger MW, Beck SC, Pereyra-Munoz N, et al. In vivo confocal imaging of the retina in animal models using scanning laser ophthalmoscopy. *Vision Res*. 2005;45:3512–3519.
27. Cordeiro MF, Guo L, Luong V, et al. Real-time imaging of single nerve cell apoptosis in retinal neurodegeneration. *Proc Natl Acad Sci U S A*. 2004;101:13352–13356.
28. Paques M, Simonutti M, Roux MJ, et al. High resolution fundus imaging by confocal scanning laser ophthalmoscopy in the mouse. *Vision Res*. 2006;46:1336–1345.
29. Eter N, Engel DR, Meyer L, et al. In vivo visualization of dendritic cells, macrophages, and microglial cells responding to laser-induced damage in the fundus of the eye. *Invest Ophthalmol Vis Sci*. 2008;49:3649–3658.
30. Criswell MH, Hu WZ, Steffens TJ, Li R, Margaron P. Comparing pegaptanib and triamcinolone efficacy in the rat choroidal neovascularization model. *Arch Ophthalmol*. 2008;126:946–952.
31. Tolentino MJ, Husain D, Theodosiadis P, et al. Angiography of fluoresceinated anti-vascular endothelial growth factor antibody and dextrans in experimental choroidal neovascularization. *Arch Ophthalmol*. 2000;118:78–84.
32. Paques M, Simonutti M, Augustin S, Goupille O, El Mathari B, Sahel JA. In vivo observation of the locomotion of microglial cells in the retina. *Glia*. 2010;58:1663–1668.
33. Grossniklaus HE, Kang SJ, Berglin L. Animal models of choroidal and retinal neovascularization. *Prog Retin Eye Res*. 2010;29:500–519.

34. Cunea A, Meyer J, Russmann C, et al. In vivo imaging with a fundus camera in a rat model of laser-induced choroidal neovascularization. *Ophthalmologica*. 2013;231:117–123.
35. Ruchatz F. Applications of Solutol HS 15- a potent solubilizer with low toxicity. *BASF ExAct*. 2002;9:6–8.
36. Kirchherr AK, Briel A, Mader K. Stabilization of indocyanine green by encapsulation within micellar systems. *Mol Pharm*. 2009;6:480–491.
37. Goody RJ, Hu W, Shafiee A, et al. Optimization of laser-induced choroidal neovascularization in African green monkeys. *Exp Eye Res*. 2011;92:464–472.
38. Hua J, Gross N, Schulze B, et al. In vivo imaging of choroidal angiogenesis using fluorescence-labeled cationic liposomes. *Mol Vis*. 2012;18:1045–1054.
39. Hughes A. A schematic eye for the rat. *Vision Res*. 1979;19: 569–588.
40. Maass A, von Leithner PL, Luong V, et al. Assessment of rat and mouse RGC apoptosis imaging in vivo with different scanning laser ophthalmoscopes. *Curr Eye Res*. 2007;32:851–861.
41. Delori F, Greenberg JP, Woods RL, et al. Quantitative measurements of autofluorescence with the scanning laser ophthalmoscope. *Invest Ophthalmol Vis Sci*. 2011;52:9379–9390.
42. McMenamin PG. Optimal methods for preparation and immunostaining of iris, ciliary body, and choroidal whole-mounts. *Invest Ophthalmol Vis Sci*. 2000;41:3043–3048.
43. Kim TH, Chen Y, Mount CW, Gombotz WR, Li X, Pun SH. Evaluation of temperature-sensitive, indocyanine green-encapsulating micelles for noninvasive near-infrared tumor imaging. *Pharm Res*. 2010;27:1900–1913.
44. Yaseen MA, Yu J, Wong MS, Anvari B. Stability assessment of indocyanine green within dextran-coated mesocapsules by absorbance spectroscopy. *J Biomed Opt*. 2007;12:064031.
45. Yaseen MA, Yu J, Jung B, Wong MS, Anvari B. Biodistribution of encapsulated indocyanine green in healthy mice. *Mol Pharm*. 2009;6:1321–1332.
46. Rodriguez VB, Henry SM, Hoffman AS, Stayton PS, Li X, Pun SH. Encapsulation and stabilization of indocyanine green within poly(styrene-alt-maleic anhydride) block-poly(styrene) micelles for near-infrared imaging. *J Biomed Opt*. 2008;13: 014025.
47. Zheng X, Xing D, Zhou F, Wu B, Chen WR. Indocyanine green-containing nanostructure as near infrared dual-functional targeting probes for optical imaging and photothermal therapy. *Mol Pharm*. 2011;8:447–456.
48. Bittner B, Gonzalez RC, Isel H, Flament C. Impact of Solutol HS 15 on the pharmacokinetic behavior of midazolam upon intravenous administration to male Wistar rats. *Eur J Pharm Biopharm*. 2003;56:143–146.
49. Seo SW, Han HK, Chun MK, Choi HK. Preparation and pharmacokinetic evaluation of curcumin solid dispersion using Solutol(R) HS15 as a carrier. *Int J Pharm*. 2012;424: 18–25.
50. Gan L, Gan Y, Zhu C, Zhang X, Zhu J. Novel microemulsion in situ electrolyte-triggered gelling system for ophthalmic delivery of lipophilic cyclosporine A: in vitro and in vivo results. *Int J Pharm*. 2008;365:143–149.

Investigative Ophthalmology & Visual Science